

## Electronic Supplementary Information

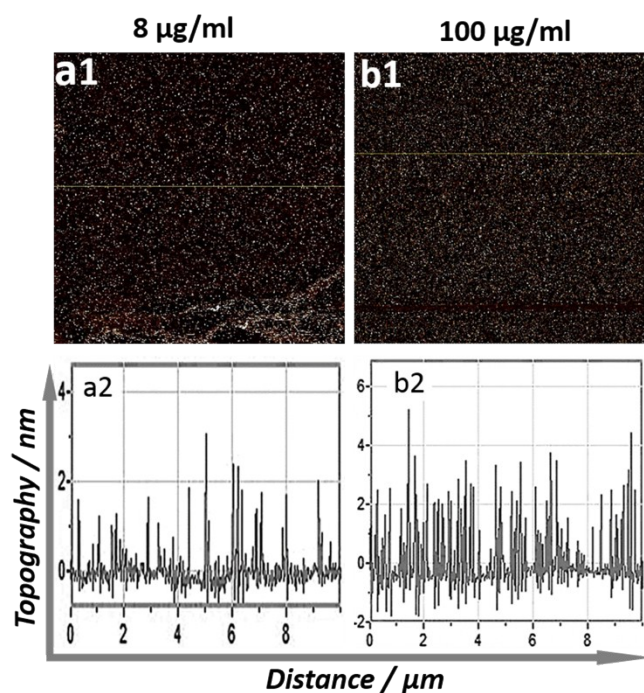
### Mono-fullerenols modulating cell stiffness by perturbing actin bundling

WeiHong Gu<sup>a,b</sup>, Xue Bai<sup>a,b</sup>, Keli Ren<sup>b,c</sup>, Xiaoyi Zhao<sup>b,d</sup>, Shibo Xia<sup>a,b</sup>, Jiaxin Zhang<sup>a,b</sup>, Yanxia Qin<sup>a</sup>, Runhong Lei<sup>a</sup>, Kui Chen<sup>a,b</sup>, Yanan Chang<sup>a</sup>, Li Zeng<sup>a</sup>, Juan Li<sup>a</sup>, Gengmei Xing<sup>a\*</sup>

#### 1. The size of fullerenols in concentration of 8 and 100 $\mu\text{g/ml}$

The diameters of fullerenols increased as the concentration rose to 8 and 100  $\mu\text{g/ml}$ .

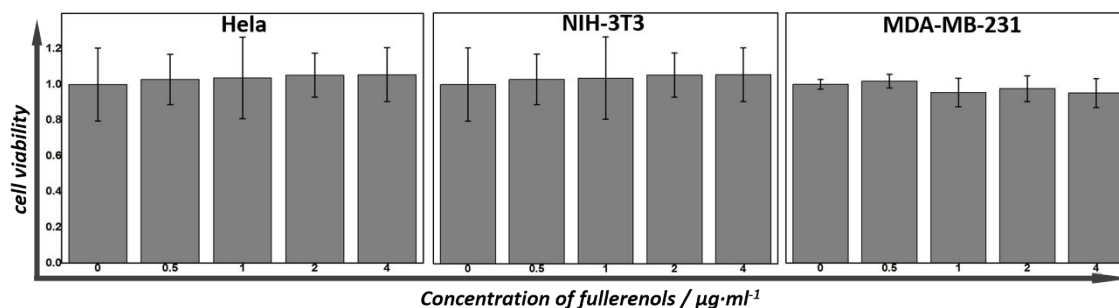
Figure S1 Diameters of fullereneol nanoparticles at higher concentrations: 8 and 100  $\mu\text{g/ml}$ . The topography images show the dispersion of fullerenols (a1, b1). The profile in a2 and b2 indicate the size of fullerenols. The image size is 10 X 10  $\mu\text{m}$ .



## 2. The viability of cells after treated by fullerenols

The cell viability have not been influenced by fullerenols (0.5~4  $\mu\text{g}/\text{ml}$ ).

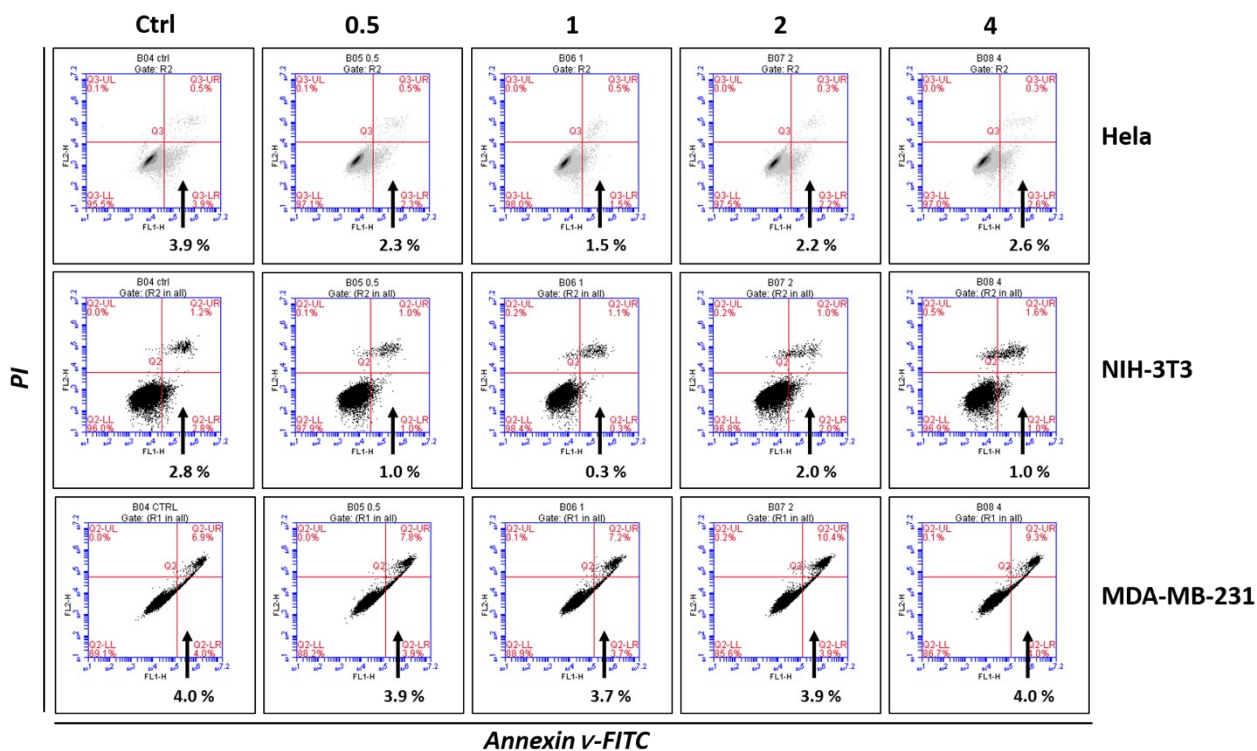
Figure S2 Effect of fullerene nanoparticles on viability of different cell lines. All of the three cell lines show normal viability compared to control groups. The data has been normalized.



## 3. Apoptosis evaluation of fullerene-treated cells

From this results, we found that fullerenols (0.5~4  $\mu\text{g}/\text{ml}$ ) would not induce apoptosis of cells.

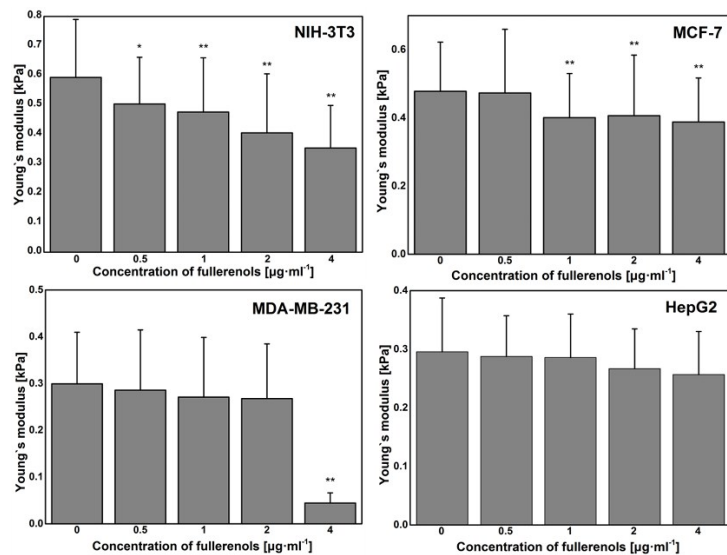
Figure S3 Apoptosis of distinct cell lines after being treated with fullerene nanoparticles. Compared with control groups in each cell lines, no apoptosis has been exacerbated.



#### 4. Stiffness of distinct cell lines

This figure presents a similar downward trend in elastic modulus after treated by fullerenols, but the specific responses differ.

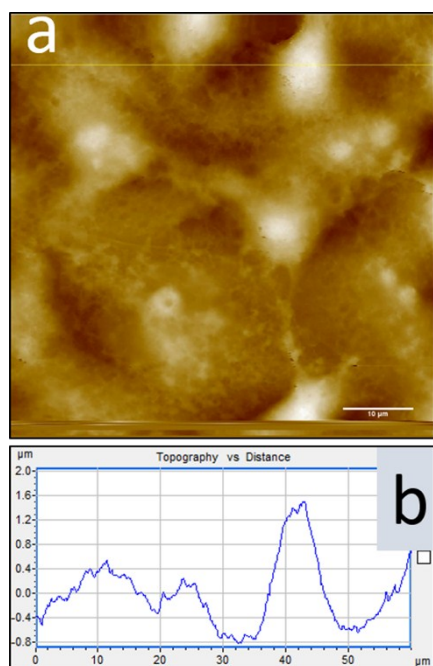
Figure S4 Alterations in stiffness of NIH-3T3, MCF-7, MDA-MB-231 and HepG2 cell lines treated with fullereneol nanoparticles. \*\* $P < 0.01$  compared with control.



#### 5. The height of adherent HeLa cells

The height of HeLa cells were measured by AFM in medium. Contact mode was used to perform the imaging.

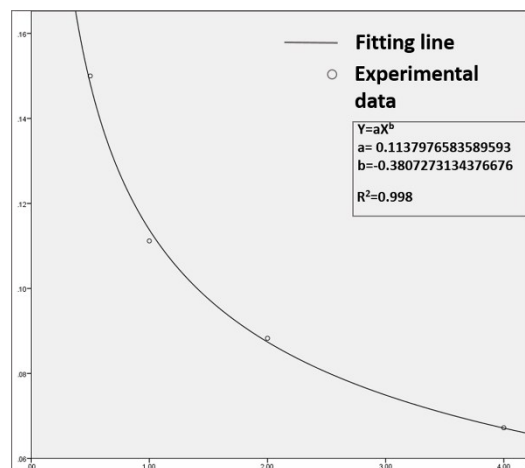
Figure S5 Height of HeLa cells in medium characterized by AFM. The topographic image (a) shows the morphology of HeLa cells in medium and the profile curve (b) is a section along the line in picture a. We can recognize that the height of a living adherent HeLa cell is about 1.5 µm.



## 6. Data fitting

Data fitting of HeLa Young's modulus was performed on SPSS and the power function is the most proper fitting.

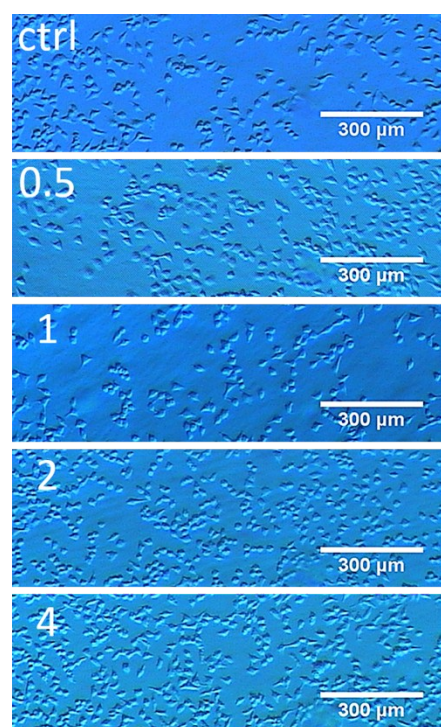
Figure S6 Power function fitting of acquired data on elastic modulus of HeLa cells. The relevant parameter are shown in the inset rectangular frame.



## 7. The morphology of HeLa cells during the acquisition of elastic modulus.

The morphology of cells during the experiment was captured with the camera integrated on the AFM.

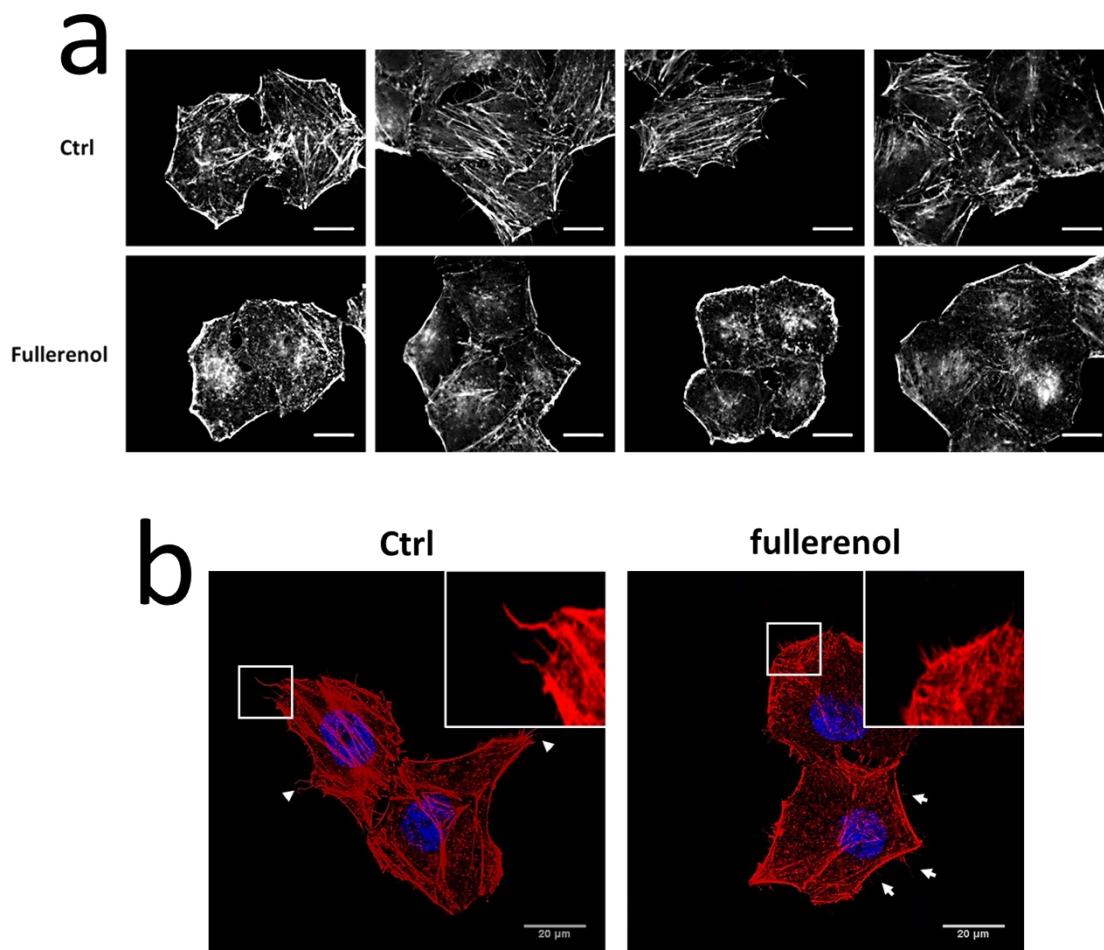
Figure S7 Images captured by the camera attached on the AFM. From the images we can see HeLa cells treated with fullereneol nanoparticles for 24 h. The scale bar = 300  $\mu\text{m}$ .



## 8. Influence of fullerenols on stress fibers and filopodia.

The figure S8 shows the decrease of stress fibers and filopodia in size and amount after treated by fullerenols

Figure S8 More images of control and treated HeLa cells are shown in a and the influence on filopodia is shown in b. Scale bar = 20  $\mu\text{m}$ .

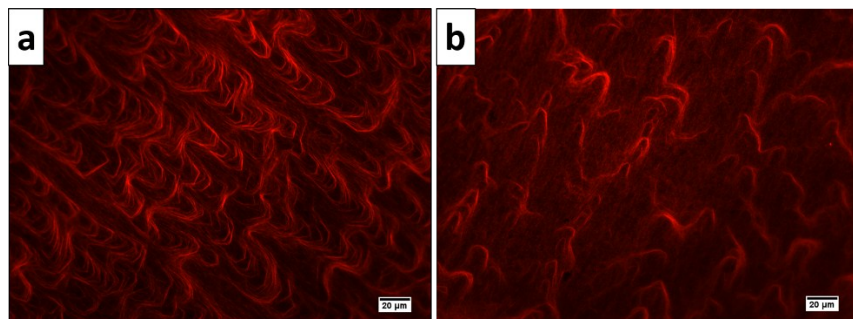




## 9. Actin bundle in vitro by inverted fluorescence microscope

The size and amount of actin bundle have been reduced under fullerenols.

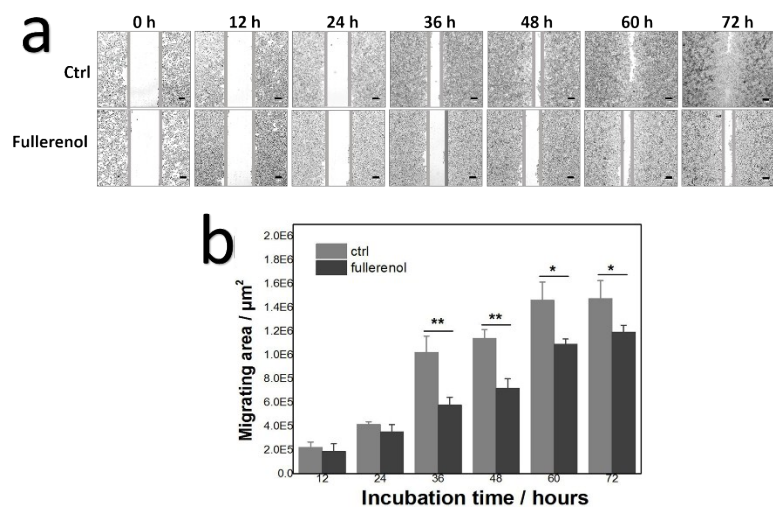
Figure S9 Effect of fullereneol nanoparticles on bundling of f-actins. The normal bundles (a) are dense and thick fibers and the affected bundles (b) are sparse and thinner. We can see a lot of far thinner fibers paving the substrate in b, while the bundles are sporadic.



## 10. Cell migrating assay

The effect of mono-fullerenols on cell migrating ability was evaluated by measuring the migrating area in wound healing assay. The results show that fullerenols (4 µg/ml) would significantly reduce the cell migration ability.

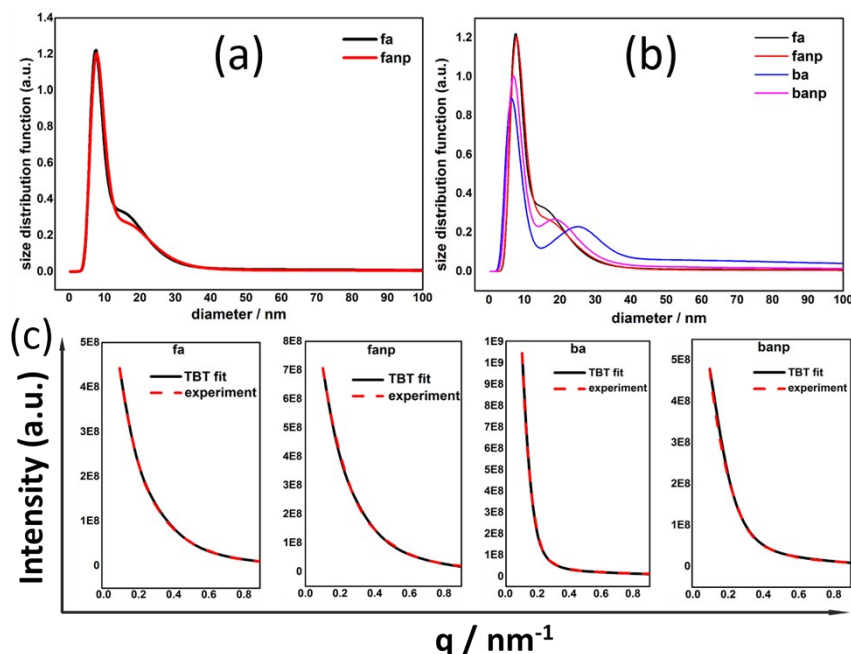
Figure S10 Effect of fullerenols on cell migrating ability. The wound healing images are shown in a (the scale bar = 200 µm). B indicates the statistical analysis of migrating area between control and fullereneol-treated group (4 µg/ml). **\*\*P<0.01, \*P<0.05**



## 11. Structural features of f-actin and b-actin characterized by SAXS.

The characterization of f-actin and b-actin by SAXS showed that fullerenols perturbed bundling without influence on polymerization. The reliability of data processing was reflected by perfect overlay of TBT and experiment data.

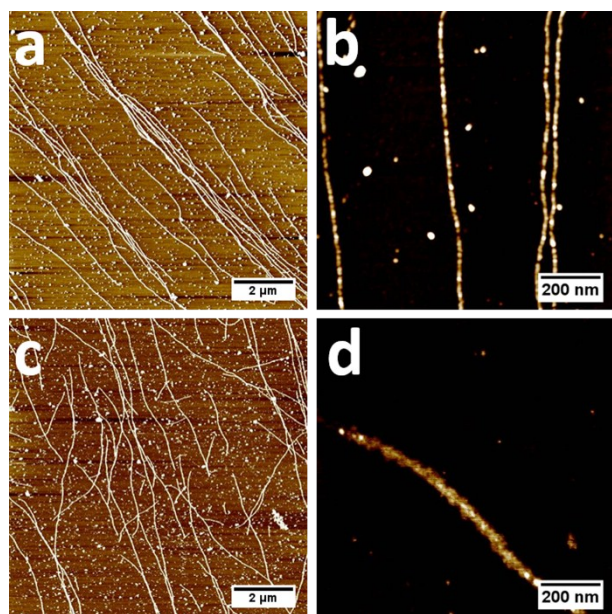
Figure S10 Size analysis of f-actin and b-actin by TBT method. Size distribution of f-actin is shown in (a). (b) gives an integral comparison of diameters. The TBT fitting results are shown in (c).



## 12. Interaction between fullerenols and f-actin

We did not capture significant distinction in polymerization between control and treated f-actin. The high resolution imaging exposed the attachment of fullerenols on f-actin.

Figure S11 Interactions between fullerenol nanoparticles and f-actins. Picture a and b are control group, while picture c and d depict the treated f-actins. The nanoparticles did not cause significant change on f-actin polymerization (a and c), but some nanoparticles have adhered to the surface of f-actins (b and d).



### 13. Calculation of fullereneol-adherent f-actin

We measured the length of a f-actin and the corresponding volume. The diameter was calculated by regarding the f-actin as a cylinder.

Figure S12 The diameter of f-actin calculated with Pico Image software. The length (a, b) and volume (c, d) of selected parts of f-actin were measured in control (a, c) and treated (b, d) groups. The corresponding values are shown in the red rectangles. The diameters of f-actin in control and treated group are calculated to be 5.6 and 6.2 nm respectively.

